2013 IEEE/RSJ International Conference on
Intelligent Robots and Systems (IROS)
November 3-7, 2013. Tokyo, Japan

Dynamic Modeling and Analysis of an Omnidirectional Mobile Robot

Chao Ren[1] and Shugen Ma[2]

Abstract— **This paper presents the dynamic modeling and analysis of a three-wheeled omnidirectional mobile robot with MY wheels-II, whose dynamics is nonlinear and piecewise-smooth. Firstly, the detailed dynamic model of the robot is derived, which shows that the robot is actually a switched non-linear system. Analysis of the robot dynamic properties based on the detailed dynamic model is presented in detail. Then to facilitate the controller design for the switched nonlinear system, based on the detailed dynamic model, an average dynamic model is proposed by simply averaging the wheel contact radius. The resulting average dynamic model is nonlinear and smooth, which may then be used as one solution for the model-based control design. Open-loop simulation results show the dynamic properties of the mobile robot. In addition, the effectiveness of the proposed average model in predicting characteristics of the detailed dynamic model is also illustrated through open-loop simulations.**

I. INTRODUCTION

Omnidirectional mobile robots (OMRs) are becoming increasingly popular in many applications, especially those in the narrow spaces, since they can perform both translational and rotational motion independently and simultaneously. In other words, they can move in any direction with any orientation angle.

Various omnidirectional wheel mechanisms were proposed in the past few decades. These mechanisms can be divided into two groups: non-switch wheels and switch wheels, depending on whether the contact radius of the wheel to the robot gravity center switches. Majority of the wheels, such as Mecanum wheel [1], Alternate wheel [2] and Ball wheel [3], are of the first group. The five switch wheel mechanisms proposed until now are shown in Fig. 1. They are Longitudinal Orthogonal-wheel [4], MY wheel [5], MY wheel-II [6], Swedish wheel [7] and Omni-wheel [8]. The dynamics of the non-switch wheeled OMRs is nonlinear and smooth while the switch wheeled OMRs are nonlinear and piecewise-smooth dynamical systems.

In our previous study, we proposed two switch wheel mechanisms, namely MY wheel [5] and MY wheel-II [6], and developed the prototype platforms. The proposed MY wheel mechanisms have several advantages over traditional wheel mechanisms, such as high payload and insensitive to fragments on the ground. However, in practice, we found that it is extremely difficult to design the controller directly based on the dynamic model due to its hybrid nature. In addition, all of the previous researches on the dynamic modeling and control are for the non-switch wheeled and Swedish wheeled

C. Ren is with Department of Robotics, Ritsumeikan University, 525-8577, Shiga, Japan gr0119vp@ed.ritsumei.ac.jp

S. Ma is with Department of Robotics, Ritsumeikan University, 525-8577, Shiga, Japan shugen@se.ritsumei.ac.jp

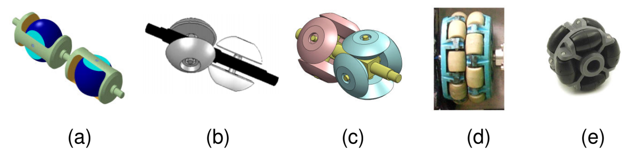

Fig. 1. Switch wheel mechanisms: (a) Longitudinal Orthogonal-wheel. (b) MY wheel. (c) MY wheel-II. (d) Swedish wheel. (e) Omni-wheel.

or Omni-wheeled OMRs, based on continuous dynamic models [9]–[13], to name a few. For the Swedish wheeled or Omni-wheeled OMRs, it is worth pointing out that the continuous dynamic models were directly employed in the previous studies by regarding it as a non-switch wheel, but no analysis was presented about the resulting modeling errors due to neglecting the switching effects.

For the switch wheeled OMRs, kinematic modeling and analysis were studied in [4], [6], [14], [15]. In [4], the kinematic model was derived for a mobile platform with three Longitudinal Orthogonal-wheel assemblies. For the same kind of omnidirectional mobile platform in [14], the average wheel contact radius was used instead of the real contact radius in the inverse kinematic model, to solve the problem of motor angular velocity fluctuations. In [6] and [15], the kinematic analysis was studied by using an optimal scale factor (OSF) instead of the average contact radius and the factors influencing the OSF were discussed. However, the dynamic modeling and analysis of the switch wheeled OMRs have not yet been studied, which are the focus of this paper.

In this paper, the dynamic modeling and analysis of a three wheeled omnidirectional mobile robot with MY wheels-II are presented. The detailed dynamic model is derived for the robot, including the motor dynamics. Then the robot dynamic properties are analyzed on the basis of the detailed dynamic model, which show that the robot is a switched nonlinear system. The average dynamic model is derived by simply using the average contact radius in the detailed dynamic model, resulting in a smooth nonlinear dynamic model. The proposed average dynamic model may be used for the model-based controller design. Finally, the robot dynamic properties and the proposed average dynamic model in predicting the behavior of the detailed dynamic model are shown through open-loop simulations.

The remainder of this paper is organized as follows. In Section II, the detailed dynamic model for a three-wheeled prototype platform is derived. The analysis of the robot dynamics is also presented. The average dynamic model is proposed in Section III. In Section IV, open-loop simulations are presented. Finally, conclusions are drawn in Section V.

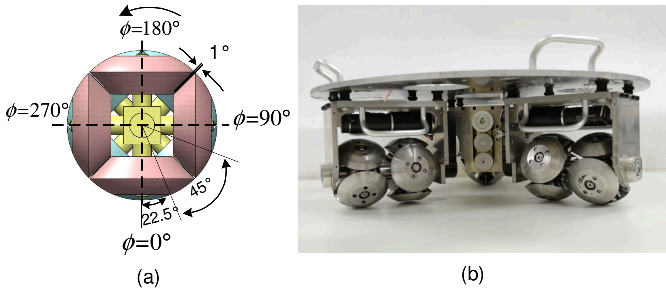

Fig. 2. (a) End view of MY wheel-II. (b) Prototype platform.

II. DETAILED DYNAMIC MODELING AND ANALYSIS

A. Detailed Dynamic Modeling

The MY wheel-II mechanism and its end view are shown in Fig. 1(c) and Fig. 2(a), respectively. The wheel consists of two balls of equal diameter on a common shaft and both balls are sliced into four spherical crowns. During the rotation of the main shaft, the two sets of crowns alternatively contact with the ground to realize continuous motion. The two contact points with ground switch between the two sets of crowns whenever the shaft turns 45°, and therefore eight switches occur during each turn (see Fig. 2(a)).

The prototype platform is shown in Fig. 2(b), with three MY wheel-II assemblies arranged at a 120° interval angle underneath the steel disk. For a detailed description of MY wheel-II mechanism and the prototype robot, we refer readers to [6].

The dynamic model is derived based on the following assumptions, which are often made in the literature [9], [10]. It is assumed that no slippage is between the wheel and the motion surface. The wheel contact friction forces in the direction perpendicular to the traction force are ignored. The friction forces on the wheel shaft and gear are viscous friction. For the dynamic modeling with static friction model (coulomb and viscous friction), we refer readers to [16] and the references therein. In addition, the motor electric circuit dynamics is neglected.

Two coordinate frames are used in the modeling (Fig. 3): the world coordinate frame $\{W\}$ which is fixed on the ground and the moving coordinate frame $\{M\}$ which is fixed on the center of gravity of the robot. The nomenclatures are defined as follows:

World coordinate frame

$\mathbf{q} = \begin{bmatrix} x & y & \theta \end{bmatrix}^T$ Robot location and orientation angle

Moving coordinate frame

$\mathbf{V}_M = \begin{bmatrix} V_x & V_y & \dot{\theta} \end{bmatrix}^T$ Robot translational velocity and rotational angular rate expressed in the moving coordinate frame

$\mathbf{F} = \begin{bmatrix} F_x & F_y \end{bmatrix}^T$ Traction force applied to the center of gravity of the robot expressed in the moving coordinate frame

T_i The traction force of each assembly, $i = 1, 2, 3$.

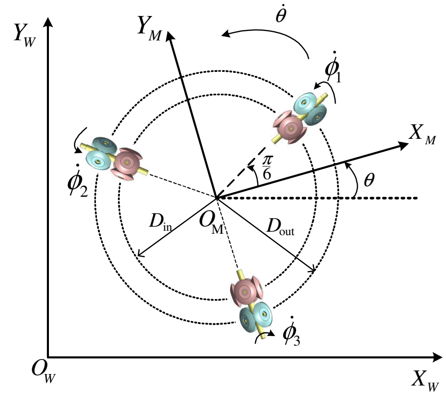

Fig. 3. Coordinate frames of the omnidirectional mobile robot.

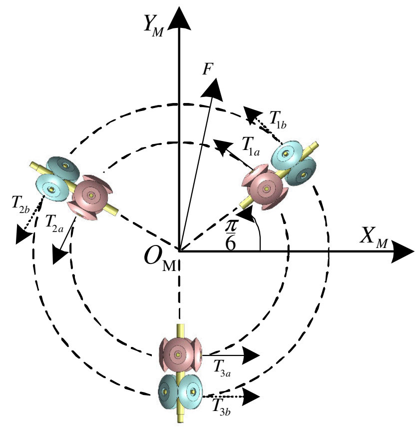

Fig. 4. Force analysis.

Mechanical constants

m	Robot mass
I_v	Robot moment of inertia
I_w	Wheel moment of inertia
R	Wheel radius
D_{in}	Inner contact radius
D_{out}	Outer contact radius
n	Gear reduction ratio

The coordinate transformation matrix from the moving coordinate frame to the world coordinate frame is as follows:

$$ {}^{W}_{M}\mathbf{R} = \begin{bmatrix} \cos\theta & -\sin\theta & 0 \\ \sin\theta & \cos\theta & 0 \\ 0 & 0 & 1 \end{bmatrix}, \tag{1} $$

and we get

$$ \dot{\mathbf{q}} = {}^{W}_{M}\mathbf{R}\mathbf{V}_M. \tag{2} $$

The dynamic properties of the mobile robot can be described with respect to the moving coordinate frame as [9] [10]:

$$ \begin{aligned} & m(\dot{V}_x - V_y\dot{\theta}) = F_x \\ & m(\dot{V}_y + V_x\dot{\theta}) = F_y \\ & I_v\ddot{\theta} = M_I \end{aligned} \tag{3} $$

where M_I is the moment of force around the axis of the robot gravity center. F_x, F_y and M_I can be obtained from Fig. 4 :

$$\begin{aligned} F_x &= -\tfrac{1}{2}T_1 - \tfrac{1}{2}T_2 + T_3 \\ F_y &= \tfrac{\sqrt{3}}{2}T_1 - \tfrac{\sqrt{3}}{2}T_2 \\ M_I &= T_1L_1 + T_2L_2 + T_3L_3 \end{aligned} \tag{4}$$

where L_i is the contact radius of each assembly, $i = 1,2,3$.

$$L_i = \begin{cases} D_{in}, & if\ \frac{\pi}{8} + \frac{n\pi}{2} < \phi_i \le \frac{3\pi}{8} + \frac{n\pi}{2} \\ D_{out}, & if -\frac{\pi}{8} + \frac{n\pi}{2} < \phi_i \le \frac{\pi}{8} + \frac{n\pi}{2} \end{cases} \quad n = 0, \pm1, \pm2, ...$$

and T_i is the traction force of each assembly, $i = 1,2,3$.

$$T_i = \begin{cases} T_{ia}, & if\ \frac{\pi}{8} + \frac{n\pi}{2} < \phi_i \le \frac{3\pi}{8} + \frac{n\pi}{2} \\ T_{ib}, & if -\frac{\pi}{8} + \frac{n\pi}{2} < \phi_i \le \frac{\pi}{8} + \frac{n\pi}{2} \end{cases} \quad n = 0, \pm1, \pm2 \dots$$

and ϕ_i is the angular position of the wheel shaft.

Combining (3) and (4), the dynamic properties of the mobile robot can be described with respect to the moving coordinate frame as [9] [10]:

$$\mathbf{M}_1\dot{\mathbf{V}}_M + \mathbf{C}_1\mathbf{V}_M = \mathbf{B}_1\mathbf{T} \tag{5}$$

where

$$\mathbf{M}_1 = \begin{bmatrix} m & 0 & 0 \\ 0 & m & 0 \\ 0 & 0 & I_v \end{bmatrix} \quad \mathbf{C}_1 = \begin{bmatrix} 0 & -m\dot{\theta} & 0 \\ m\dot{\theta} & 0 & 0 \\ 0 & 0 & 0 \end{bmatrix}$$

$$\mathbf{B}_1 = \begin{bmatrix} -\frac{1}{2} & -\frac{1}{2} & 1 \\ \frac{\sqrt{3}}{2} & -\frac{\sqrt{3}}{2} & 0 \\ L_1 & L_2 & L_3 \end{bmatrix} \mathbf{T} = \begin{bmatrix} T_1 & T_2 & T_3 \end{bmatrix}^T.$$

The motors dynamics can be described as follows:

$$I_0\dot{\omega} + (b_0 + \frac{k_t k_b}{R_a})\omega + \frac{R}{n}\mathbf{T} = \frac{k_t}{R_a}\mathbf{u} \tag{6}$$

where $\omega = \begin{bmatrix} \omega_1 & \omega_2 & \omega_3 \end{bmatrix}^T$, $\mathbf{u} = \begin{bmatrix} u_1 & u_2 & u_3 \end{bmatrix}^{\mathrm{T}}$. ω_i is the motor angular rate, u_i is the applied motor voltage, R_a is the armature resistance, k_b is the motor back emf constant, k_t is the motor torque constant, I_0 is the combined moment of inertia of the motor, gear train and wheel referred to the motor shaft, b_0 is the combined viscous friction coefficient of the motor, gear and wheel shaft, and n is the gear reduction ratio.

The kinematic relationship with respect to the moving coordinate frame is given by (see Fig. 3):

$$\dot{\mathbf{\Phi}} = \frac{1}{R}\mathbf{J}_M\mathbf{V}_M \tag{7}$$

$$\omega = n\dot{\mathbf{\Phi}} \tag{8}$$

where $\dot{\mathbf{\Phi}} = \begin{bmatrix} \dot{\phi}_1 & \dot{\phi}_2 & \dot{\phi}_3 \end{bmatrix}^T$, $\mathbf{J}_M = \begin{bmatrix} -\frac{1}{2} & \frac{\sqrt{3}}{2} & L_1 \\ -\frac{1}{2} & -\frac{\sqrt{3}}{2} & L_2 \\ 1 & 0 & L_3 \end{bmatrix}$.

From (5)-(8), we obtain the dynamic model of the mobile robot expressed in the moving coordinate frame:

$$\mathbf{M}_2\dot{\mathbf{V}}_M + \mathbf{C}_2\mathbf{V}_M = \mathbf{B}_2\mathbf{u} \tag{9}$$

where

$\mathbf{M}_2 =$

$$\begin{bmatrix} \frac{3}{2}p_0 + m & 0 & p_0(-\frac{L_1+L_2-2L_3}{2}) \\ 0 & \frac{3}{2}p_0 + m & \frac{\sqrt{3}}{2}p_0(L_1 - L_2) \\ p_0(-\frac{L_1+L_2-2L_3}{2}) & \frac{\sqrt{3}}{2}p_0(L_1 - L_2) & p_0(L_1^2 + L_2^2 + L_3^2) + I_v \end{bmatrix}$$

$\mathbf{C}_2 =$

$$\begin{bmatrix} \frac{3}{2}p_1 & -m\dot{\theta} & p_1(-\frac{L_1+L_2-2L_3}{2}) \\ m\dot{\theta} & \frac{3}{2}p_1 & \frac{\sqrt{3}}{2}p_1(L_1 - L_2) \\ p_1(-\frac{L_1+L_2-2L_3}{2}) & \frac{\sqrt{3}}{2}p_1(L_1 - L_2) & p_1(L_1^2 + L_2^2 + L_3^2) \end{bmatrix}$$

$$\mathbf{B}_2 = p_2\begin{bmatrix} -\frac{1}{2} & -\frac{1}{2} & 1 \\ \frac{\sqrt{3}}{2} & -\frac{\sqrt{3}}{2} & 0 \\ L_1 & L_2 & L_3 \end{bmatrix}$$

$p_0 = \frac{n^2 I_0}{R^2}$, $p_1 = \frac{n^2}{R^2}(b_0 + \frac{k_t k_b}{R_a})$, $p_2 = \frac{n k_t}{R R_a}$.

Finally, the robot dynamic model in the world coordinate frame can be obtained by combining (1), (2) and (9):

$$\mathbf{M}\ddot{\mathbf{q}} + \mathbf{C}\dot{\mathbf{q}} = \mathbf{B}\mathbf{u} \tag{10}$$

where
$\mathbf{M} = \mathbf{M}_2{}_M^W\mathbf{R}^T$, $\mathbf{C} = \mathbf{C}_2{}_M^W\mathbf{R}^T - \mathbf{M}_2{}_M^W\mathbf{R}^T{}_M^W\dot{\mathbf{R}}{}_M^W\mathbf{R}^T$, $\mathbf{B} = \mathbf{B}_2$.

B. Analysis

As one MY wheel-II assembly has two contact modes with the ground, i.e., inner wheel contact with contact radius D_{in} and outer wheel contact with contact radius D_{out}, the mobile robot with three MY wheel-II assemblies has eight contact modes in total. The contact modes are listed in Table I. Each contact mode corresponds to a smooth nonlinear robot dynamical subsystem. Therefore, the robot dynamics has eight nonlinear smooth dynamical subsystems in total and switches between these subsystems, i.e., a switched nonlinear system, which can also be derived from (9). It should be pointed out that not all of the eight contact modes always appear in the robot motion. It depends on the robot trajectory, initial wheel position, which can be derived by detailed analysis using the robot kinematic equation. In addition, for a mobile robot with four MY wheel-II assemblies, the robot will have sixteen smooth nonlinear dynamical subsystems in total.

As also shown in (9) and (10), the mobile robot with MY wheels-II is a piecewise-smooth nonlinear dynamical system or hybrid system. The smoothness is lost only at the instantaneous and discrete switching events. The timescales over which transitions of switch occur in the robot system are remarkably small compared with that of the overall dynamics. In addition, the robot dynamical system can also be considered as continuous-time dynamical system with discrete switch events [17].

Moreover, switched systems are a class of hybrid dynamical systems consisting of a family of subsystems, and a rule (i.e., switching signal) that orchestrates the switching between them [17]. For the switch wheeled OMRs, as shown

TABLE I

CONTACT MODES OF THE THREE-WHEELED MOBILE ROBOT

L_1, L_2, L_3	D_{in}, D_{in}, D_{in}	D_{in}, D_{in}, D_{out}	D_{in}, D_{out}, D_{in}	D_{in}, D_{out}, D_{out}
Contact Mode	Mode 1	Mode 2	Mode 3	Mode 4
L_1, L_2, L_3	D_{out}, D_{in}, D_{in}	D_{out}, D_{in}, D_{out}	D_{out}, D_{out}, D_{in}	$D_{out}, D_{out}, D_{out}$
Contact Mode	Mode 5	Mode 6	Mode 7	Mode 8

in (9) and (10), the switching signal is the wheel contact radius, i.e., $\mathbf{L} = \begin{bmatrix} L_1 & L_2 & L_3 \end{bmatrix}^T$. It is worth pointing out that the switching signal depends simultaneously on the contact radius of the three wheels, i.e., the vector $\mathbf{L}$. In other words, the current active subsystem is determined by the value of L_1, L_2 and L_3. For instance, at one time instant, if the contact radius of the three wheels is $\mathbf{L} = \begin{bmatrix} D_{in} & D_{in} & D_{in} \end{bmatrix}^T$, it can be seen from Table I that the current active subsystem is Mode 1.

Finally, it can be seen from (4), (9) and (10) that the mobile robot is a smooth and linear dynamical system if the robot moves without rotation. More importantly, although the mobile robot has eight contact modes regardless of whether the robot rotates, it is worth noting that the nonlinearity and switching of the dynamics are introduced only when the robot rotates.

Remark 1: For the five switch wheel mechanisms shown in Fig. 1, regardless of the number of switches encountered by the wheel contact radius during each turn of the wheel, all of the three-wheeled OMRs based on any of the five switch wheels have only eight subsystems in total. This is because each of the five switch wheel mechanisms has only two contact modes. However, the switches of the wheel contact radius during each wheel turn will influence the switching frequency of the subsystems. For instance, as shown in Fig. 1, the Swedish wheel has the maximum of switches in each turn. Note that the switching frequency of the robot subsystems may influence the control system performance.

III. AVERAGE DYNAMIC MODELING

Define $\bar{\mathbf{q}} = \begin{bmatrix} \bar{x} & \bar{y} & \bar{\theta} \end{bmatrix}$ as the robot position and orientation vector in the average model. The average dynamic model can be easily derived from (10) by choosing

$$L_i = L_a = \frac{D_{in} + D_{out}}{2} \quad i = 1, 2, 3.$$

The obtained average dynamic model is as follows:

$$\mathbf{M}_a \ddot{\bar{\mathbf{q}}} + \mathbf{C}_a \dot{\bar{\mathbf{q}}} = \mathbf{B}_a \mathbf{u} \tag{11}$$

where

$$\mathbf{M}_a = \mathbf{M}_{2a} {}_M^W\bar{\mathbf{R}}_a^T,\ \mathbf{C}_a = \mathbf{C}_{2a} {}_M^W\bar{\mathbf{R}}_a^T - \mathbf{M}_{2a} {}_M^W\bar{\mathbf{R}}_a^T {}_M^W\dot{\bar{\mathbf{R}}}_a {}_M^W\bar{\mathbf{R}}_a^T,$$

$$\mathbf{M}_{2a} = \begin{bmatrix} \frac{3}{2}p_0 + m & 0 & 0 \\ 0 & \frac{3}{2}p_0 + m & 0 \\ 0 & 0 & 3p_0 L_a^2 + I_v \end{bmatrix}$$

$$\mathbf{C}_{2a} = \begin{bmatrix} \frac{3}{2}p_1 & -m\dot{\bar{\theta}} & 0 \\ m\dot{\bar{\theta}} & \frac{3}{2}p_1 & 0 \\ 0 & 0 & 3p_1 L_a^2 \end{bmatrix}$$

$$\mathbf{B}_a = p_2 \begin{bmatrix} -\frac{1}{2} & -\frac{1}{2} & 1 \\ \frac{\sqrt{3}}{2} & -\frac{\sqrt{3}}{2} & 0 \\ L_a & L_a & L_a \end{bmatrix}$$

$${}_m^w\bar{\mathbf{R}}_a = \begin{bmatrix} \cos\bar{\theta} & -\sin\bar{\theta} & 0 \\ \sin\bar{\theta} & \cos\bar{\theta} & 0 \\ 0 & 0 & 1 \end{bmatrix}$$

and p_0, p_1 and p_2 are the same as those in (9).

The detailed dynamic model (10) can be rewritten as:

$$\ddot{\mathbf{q}} = \mathbf{f}(t) + \mathbf{g}(t) \tag{12}$$

where

$$\mathbf{f}(t) = -\mathbf{M}_a^{-1}\mathbf{C}_a\dot{\mathbf{q}} + \mathbf{M}_a^{-1}\mathbf{B}_a\mathbf{u}$$
$$\mathbf{g}(t) = -(\mathbf{M}^{-1}\mathbf{C} - \mathbf{M}_a^{-1}\mathbf{C}_a)\dot{\mathbf{q}} + (\mathbf{M}^{-1}\mathbf{B} - \mathbf{M}_a^{-1}\mathbf{B}_a)\mathbf{u}.$$

Therefore, system (12) can be considered as a perturbed system. The average dynamic model (11) is viewed as the nominal model and the perturbation term $\mathbf{g}(t)$ represents the modeling error against the detailed model. Obviously, a small $\mathbf{g}(t)$ is required to guarantee the effectiveness of the average dynamic model in the prediction of the detailed dynamic model. In addition, $\mathbf{g}(t)$ is robot velocity and control input dependent. Therefore, the robot trajectory has influences on the modeling error of the average dynamic model, which is also shown in the open-loop simulations in the next Section. Furthermore, the mechanical parameters, such as the wheel contact radius D_{in} and D_{out}, the wheel radius R and the gear reduction ratio n, also have influences on the modeling error.

Moreover, the derived average dynamic model (11) is nonlinear and smooth, ignoring the switching effects. Thereby, it predicts the average behavior of the detailed dynamic model. In addition, the control system may then be designed based on the average dynamic model, wherein the modeling errors including $\mathbf{g}(t)$ can be viewed as perturbations and compensated by the controller. However, if the switching effects can not be completely compensated in the controller, the average dynamic model based control design will lead to slight robot vibrations due to the switching effects.

IV. OPEN-LOOP SIMULATIONS

Typically, time-domain model validation is performed by comparing the time-response of both models to the same input command [18]. Therefore, the dynamic properties of the robot and the effectiveness of the proposed average dynamic model in predicting the average behavior of the detailed dynamic model are demonstrated through open-loop simulations. The simulation process is shown in Fig. 5, and was implemented in Matlab/Simulink. The control

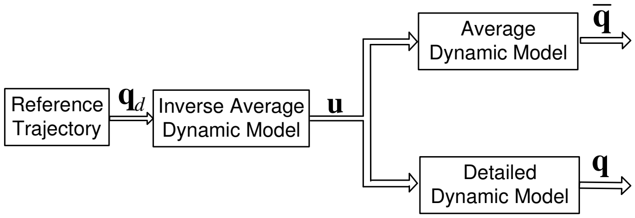

Fig. 5. Open-loop simulation process.

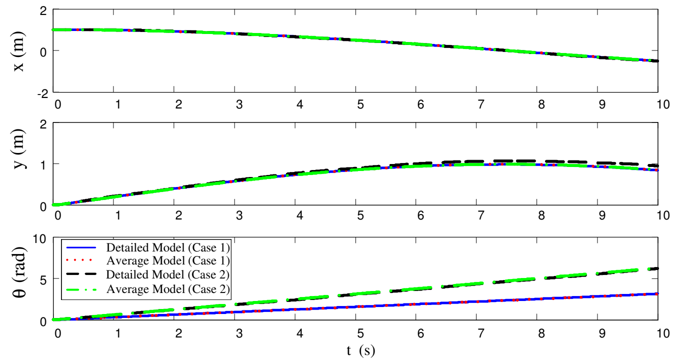

Fig. 6. Trajectory of the detailed model and average model in x, y, θ, respectively.

input signal was obtained by using the inverse dynamics of the average model, and was then given to both models. In addition, because the proposed average dynamic model is derived from the detailed dynamic model, it only approaches the detailed model in terms of accuracy.

The parameter values in the simulation are as follows: $m = 33\,\mathrm{kg}$, $I_v = 1.35\ \mathrm{kg\cdot m^2}$,$R = 0.06\,\mathrm{m}$, $D_{in} = 0.2\,\mathrm{m}$, $D_{out} = 0.3\,\mathrm{m}$, $I_0 = 9.7\times10^{-6}\ \mathrm{kg\cdot m^2}$, $k_t = 0.0292\,\mathrm{N\cdot m/A}$, $k_b = 328$ rpm/V, $n = 30$, $b_0 = 6\times10^{-5}$ Nms/rad, $R_a = 0.61\ \Omega$. The robot initial position and orientation is set as $\begin{bmatrix} 1\,\mathrm{m} & 0\,\mathrm{m} & 0\,\mathrm{rad} \end{bmatrix}$.

In the simulations, two reference circle trajectories with different robot rotational velocities are employed. The equations of the reference trajectory are as follows:

$$\begin{aligned} x_d &= r\cos(\alpha t) \\ y_d &= r\sin(\alpha t) \\ \theta_d &= \beta t \end{aligned}$$

The trajectory parameters for two cases are chosen as follows:

Case 1: $r = 1$ m, $\alpha=\frac{\pi}{15}$ rad/s, $\beta=\frac{\pi}{10}$ rad/s.

Case 2: $r = 1$ m, $\alpha=\frac{\pi}{15}$ rad/s, $\beta=\frac{\pi}{5}$ rad/s.

The simulation results are shown in Fig. 6 - Fig. 10. It can be seen from Fig. 6 and Fig. 7 that the robot position of the proposed average model has a good agreement with the detailed dynamic model for different control inputs. However, it is observed that the performance of the average model with Case 1 is better than that with Case 2. This is possibly due to the fact that the modeling error $\mathbf{g}(t)$ in (12) is robot velocity and control input dependent. Therefore, for different robot trajectories, the performance of the average modeling method will be different.

It can be seen from Fig. 8 that the robot translational

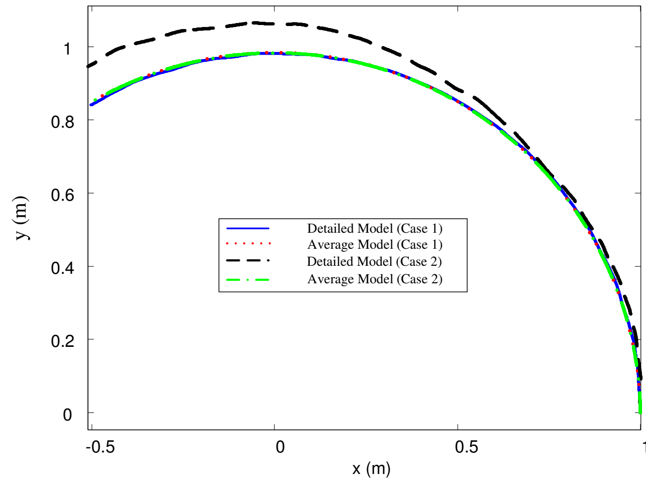

Fig. 7. Trajectory of the detailed model and average model.

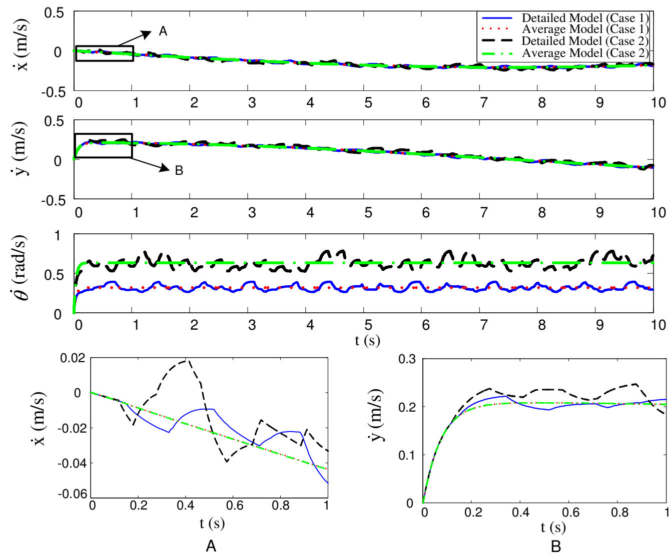

Fig. 8. Robot velocity of the detailed model and average model.

and rotational velocities have fluctuations. This is because the mobile robot is switched nonlinear system. The applied motor voltage is smooth and is derived from the inverse average model and thus switching effects are neglected, i.e., no compensation of the switching effects is considered in the applied motor voltage (see Fig. 9 of Case 1). Therefore, the robot vibrations can be reduced by designing separate controllers for each subsystem, which, however, will be much more complicated in the controller design due to the stability problem [17]. Moreover, it can also be observed in Fig. 8 that the response of the average model is smooth due to the neglecting of switching effects against the detailed model. Besides, the average dynamic model is able to approximate the average behavior of the detailed dynamic model.

Finally, Fig. 10 shows the wheel contact radius (the switching signal) of Case 1. We can see that the modeling error arises from the fact that the average contact radius (dashed line) is inaccurate in predicting the real wheel

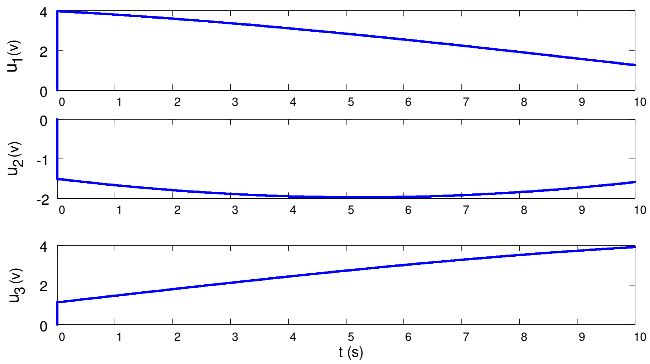

Fig. 9. The applied motor voltage of Case 1.

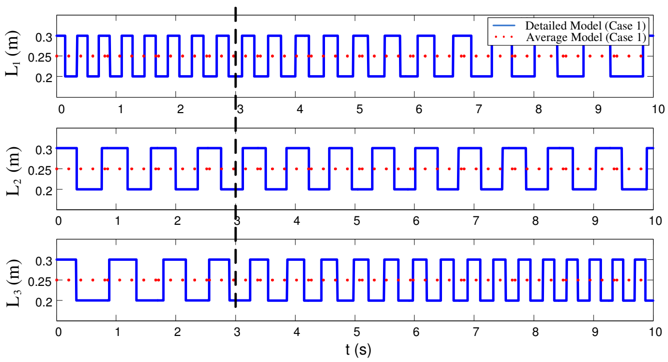

Fig. 10. Contact radius of the detailed model and average model.

contact radius (solid line). In addition, it is shown in Fig. 10 that the switching signal is determined simultaneously by the three contact radius L_i. For example, at the time $t = 3$ s, the contact radius of the three wheels are $\mathbf{L}_{(t=3\ \mathrm{s})} = \begin{bmatrix} D_{in} & D_{in} & D_{in} \end{bmatrix}^T$. Thus, from Table I, it can be seen that the active subsystem at $t = 3$ s is Mode 1.

V. CONCLUSIONS

In this paper, the dynamic modeling and analysis of a three-wheeled omnidirectional mobile robot with MY wheels-II have been presented. Firstly, the detailed dynamic model including the motor dynamics has been derived. It is shown in the detailed dynamic model that the dynamics of the mobile robot has eight smooth nonlinear dynamical subsystems in total, i.e., a switched nonlinear system. The switching signal of the switched nonlinear system is determined simultaneously by the contact radius of the three wheels. Then to facilitate the model-based controller design for the mobile robot, a smooth nonlinear average dynamic model derived from the detailed dynamic model has been proposed, ignoring the switching effects. The main advantages of the proposed average model is easy to be derived and implemented. It is shown in the simulations that the robot will have vibrations if no compensation of the switching effects is considered in the applied motor voltage. In addition, it is also shown that the proposed average dynamic model is effective in approximating the average dynamics of the detailed model. Finally, the proposed dynamic modeling and analysis can be easily extended to other switch wheeled OMRs.

In the future, the influences on the average modeling error, such as the robot trajectory and mechanical design parameters, will be studied in detail.

REFERENCES

[1] B. Ilou, "Wheels for a course stable self-propelling vehicle movable in any desired direction on the ground or some other base," Patent U.S. Patent 3 876 255, Apr 8, 1975.

[2] K.-S. Byun and J.-B. Song, "Design and construction of continuous alternate wheels for an omnidirectional mobile robot," *J. Robot. Syst.*, vol. 20, no. 9, pp. 569–579, 2003.

[3] K. Tadakuma and R. Tadakuma, "Mechanical design of "omni-ball": Spherical wheel for holonomic omnidirectional motion," in *Proc. IEEE Int. Conf. Automation Sci. and Eng.*, Sept. 2007, pp. 788 –794.

[4] F. Pin and S. Killough, "A new family of omnidirectional and holonomic wheeled platforms for mobile robots," *IEEE Trans. Robot. Autom.*, vol. 10, no. 4, pp. 480 –489, Aug. 1994.

[5] C. Ye and S. Ma, "Development of an omnidirectional mobile platform," in *Proc. IEEE Int. Conf. Mechatronics and Automation*, Changchun, China, Aug. 2009, pp. 1111 –1115.

[6] S. Ma, C. Ren, and C. Ye, "An omnidirectional mobile robot: Concept and analysis," in *Proc. 2012 IEEE Int. Conf. Robotics and Biomimetics*, Guangzhou, China, pp. 920–925.

[7] G. Indiveri, "Swedish wheeled omnidirectional mobile robots: Kinematics analysis and control," *IEEE Trans. Robot.*, vol. 25, no. 1, pp. 164 –171, Feb. 2009.

[8] H. Asama *et al*, "Development of an omni-directional mobile robot with 3 dof decoupling drive mechanism," in *Proc. IEEE Int. Conf. Robotics and Automation*, vol. 2, 1995, pp. 1925–1930.

[9] K. Watanabe, Y. Shiraishi, S. Tzafestas, J. Tang, and T. Fukuda, "Feedback control of an omnidirectional autonomous platform for mobile service robots," *J. Intell. Robot. Syst.*, vol. 22, pp. 315–330, 1998.

[10] Y. Liu, J. J. Zhu, R. L. W. II, and J. Wu, "Omni-directional mobile robot controller based on trajectory linearization," *Robot. Auton. Syst.*, vol. 56, no. 5, pp. 461 – 479, 2008.

[11] K. Kanjanawanishkul and A. Zell, "Path following for an omnidirectional mobile robot based on model predictive control," in *Proc. IEEE Int. Conf. Robotics and Automation*, Kobe, Japan, May 2009, pp. 3341 –3346.

[12] K.-Y. Tu, "A linear optimal tracker designed for omnidirectional vehicle dynamics linearized based on kinematic equations," *Robotica*, vol. 28, pp. 1033–1043, 2010.

[13] H.-C. Huang, C.-C. Tsai, and S.-C. Lin, "Adaptive polar-space motion control for embedded omnidirectional mobile robots with parameter variations and uncertainties," *J. Intell. Robot. Syst.*, vol. 62, pp. 81–102, 2011.

[14] G. Mourioux, C. Novales, G. Poisson, and P. Vieyres, "Omni-directional robot with spherical orthogonal wheels: concepts and analyses," in *Proc. IEEE Int. Conf. Robotics and Automation*, Florida, USA, May. 2006, pp. 3374 –3379.

[15] C. Ye, H. Li, and S. Ma, "Kinematic analysis of an omnidirectional mobile robot with my wheels," in *Proc. IEEE Int. Conf. Robotics and Biomimetics*, Phucket, Thailand, Dec. 2011, pp. 1748 –1753.

[16] A. Conceicao, A. Moreira, and P. Costa, "Practical approach of modeling and parameters estimation for omnidirectional mobile robots," *IEEE/ASME Trans. Mechatronics*, vol. 14, no. 3, pp. 377–381, 2009.

[17] D. Liberzon, *Switching in Systems and Control*. Berlin, Germany: Birkhauser, 2003.

[18] J. Martins, Z. Mohamed, M. Tokhi, J. Sa da Costa, and M. Botto, "Approaches for dynamic modelling of flexible manipulator systems," *Proc. IEE Control Theory Applicat.*, vol. 150, no. 4, pp. 401–411, 2003.